

An equilibrium statistical model for the spreading phase of open-ocean convection

MARK T. DiBATTISTA AND ANDREW J. MAJDA[†]

Courant Institute of Mathematical Sciences, New York University, New York, NY 10012

Contributed by Andrew J. Majda, March 3, 1999

ABSTRACT A “most probable state” equilibrium statistical theory for random distributions of hetons in a closed basin is developed here in the context of two-layer quasigeostrophic models for the spreading phase of open-ocean convection. The theory depends only on bulk conserved quantities such as energy, circulation, and the range of values of potential vorticity in each layer. The simplest theory is formulated for a uniform cooling event over the entire basin that triggers a homogeneous random distribution of convective towers. For a small Rossby deformation radius typical for open-ocean convection sites, the most probable states that arise from this theory strongly resemble the saturated baroclinic states of the spreading phase of convection, with a stabilizing barotropic rim current and localized temperature anomaly.

Open-ocean deep convection, which occurs in the Labrador Sea, the Greenland Sea, and the Mediterranean Sea in the current world climate, is an important phenomenon that strongly influences the thermohaline circulation governing the poleward transport of heat in the ocean. These basins with open-ocean convection are characterized by a small Rossby deformation radius compared with the basin scale so that rotational effects become important on comparatively small length scales. For a recent comprehensive survey, see the review in ref. 1.

One important aspect of open-ocean convection is the spreading of heat and vorticity throughout the ocean interior in response to strong surface cooling. It is obviously an interesting problem to develop simplified statistical theories that predict the extent and structure of the spreading phase of open-ocean convection without resolving the fine-structure details of the dynamics but rely only on bulk conserved quantities such as energy and circulation. Such theories potentially can yield effective parametrization of the mesoscale effects of open-ocean convection in ocean general circulation models.

Here, we develop an equilibrium statistical model for the spreading phase of open-ocean convection and analyze its predictions in the context of localized temperature anomalies, which are called hetons (2), for the two-layer quasigeostrophic equations (3–5). In this model, random distributions of elementary hetons mimic the geostrophically balanced response to convective mixing forced by surface cooling. The hetons model the localized exchange of mass between the two layers in the fluid, which raises the interface between the colder water below and the warmer water above. We find that the equilibrium statistical theory predicts a cold temperature anomaly confined within a barotropic rim current, which is in qualitative agreement with numerical integration of heton models (3–5).

After preliminary background discussion on the two-layer quasigeostrophic equations, we introduce the “most probable state” equilibrium statistical theory. This theory involves

a “maximum-entropy” principle that utilizes only a few judiciously chosen physical constraints involving the total energy, the total circulation in each layer, and the *a priori* extrema of potential vorticity in each layer. The statistical theory yields specific equilibrium solutions of the inviscid two-layer quasigeostrophic equations that represent the most probable mean-field large-time response to a statistical ensemble of hetons generated by a surface cooling event. Conditions guaranteeing the nonlinear (and linearized) stability of the mean-field statistical steady states are applied throughout the paper. There is both rigorous mathematical (6, 7) and computational evidence in more idealized settings (8, 9) for the validity and utility of the predictions of such a statistical theory employing these constraints.

Two-Layer Quasigeostrophic Formalism

Specifically, the quasigeostrophic fluid model treated in this paper is comprised of two stably stratified layers that evolve in a unit basin with extent $-1/2 < x < 1/2$ and $-1/2 < y < 1/2$. The two layers are assumed to have constant density and identical depth so that F , the “rotational Froude number,” is the same for both layers (10). The potential vorticities of the upper and lower layers, q_1 and q_2 , and the upper and lower layer stream functions, ψ_1 and ψ_2 , are coupled through the relations

$$\begin{aligned} q_1 &= \Delta\psi_1 - F(\psi_1 - \psi_2) \\ q_2 &= \Delta\psi_2 + F(\psi_1 - \psi_2). \end{aligned} \quad [1]$$

The nondimensional parameter F is the square of the ratio of length scales, $F = 1/L_R^2$, where L_R is the Rossby deformation radius nondimensionalized by the (unit) basin length scale. The dynamic equation for the two-layer fluid is expressed by the material conservation of potential vorticity in each layer,

$$\begin{aligned} \frac{\partial q_1}{\partial t} + \nabla^\perp \psi_1 \cdot \nabla q_1 &= 0 \\ \frac{\partial q_2}{\partial t} + \nabla^\perp \psi_2 \cdot \nabla q_2 &= 0, \end{aligned} \quad [2]$$

together with the conditions of no normal flow at the lateral boundaries of the basin. Here, and throughout the paper, upper-layer quantities are designated by subscript 1, and lower-layer quantities by subscript 2.

It is well known that the system of equations in 2 conserves the energy,

$$E = - \sum_{j=1}^2 \int q_j \psi_j dA, \quad [3]$$

the circulations in each layer,

$$\Gamma_j = \int q_j dA, \quad j = 1, 2, \quad [4]$$

The publication costs of this article were defrayed in part by page charge payment. This article must therefore be hereby marked “advertisement” in accordance with 18 U.S.C. §1734 solely to indicate this fact.

PNAS is available online at www.pnas.org.

[†]To whom reprint requests should be addressed. e-mail: jonjon@cims.nyu.edu.

and, indeed, any arbitrary function \mathcal{G} of the potential vorticity in each layer,

$$\int \mathcal{G}(q_j) dA, \quad j = 1, 2. \tag{5}$$

This last family of conserved quantities in **5** is a consequence of the material conservation of potential vorticity in each layer.

It is natural to decompose the stream functions of a two-layer fluid into barotropic and baroclinic components, ψ_B and ψ_T ,

$$\begin{aligned} \psi_B &= \frac{\psi_1 + \psi_2}{\sqrt{2}} \\ \psi_T &= \frac{\psi_1 - \psi_2}{\sqrt{2}}. \end{aligned} \tag{6}$$

The barotropic component therefore measures the part of the flow that is common to both layers, while the baroclinic component measures the part of the flow due to vertical shear.

The temperature anomaly can be shown to depend entirely on the baroclinic component of the stream function (10),

$$-F\psi_T. \tag{7}$$

Thus, a perturbation that pushes the fluid interface upward and establishes a local maximum displaces the warmer fluid in the upper layer with colder fluid from the lower layer, lowering the average temperature in the fluid column. This configuration, which is essentially a heton, is associated with a cyclonic vortex in the upper layer and a matching anticyclonic vortex in the lower layer.

The energy in a two-layer model, with nonzero F , can be partitioned among three distinct components, one that is entirely barotropic—the barotropic kinetic energy—and two that depend on the baroclinic fields—the baroclinic kinetic energy and the potential energy. Given the decomposition defined above in **6**, the total energy, E , is conserved,

$$E = E_B + K_T + P, \tag{8}$$

where the energy components are defined by

$$\begin{aligned} \text{Barotropic Kinetic} \quad E_B &= \frac{1}{2} \int |\nabla\psi_B|^2 \\ \text{Baroclinic Kinetic} \quad E_T &= \frac{1}{2} \int |\nabla\psi_T|^2 \\ \text{Potential} \quad P &= F \int \psi_T^2. \end{aligned} \tag{9}$$

The Link Between Equilibrium Statistical Theories and Heton Models for Open-Ocean Convection

An elementary heton (2) is a purely baroclinic structure with potential vorticity having the form

$$\begin{aligned} q_1(\mathbf{x}) &= \Delta q_i \delta_{\mathbf{x}_i} \\ q_2(\mathbf{x}) &= (-\Delta q_i) \delta_{\mathbf{x}_i}, \end{aligned} \tag{10}$$

where $\Delta q_i > 0$ is the strength of the i th heton, $\mathbf{x}_i = (x_i, y_i)$ is a random location in the basin, and $\delta_{\mathbf{x}}$ is the Dirac delta function at \mathbf{x} . Such elementary hetons in **10** are introduced in ref. 3 to model the geostrophically balanced response to the small-scale convective mixing resulting from local surface cooling.

In basins with small Rossby deformation radii—i.e., with $L_R \ll 1$, where $L_R = \sqrt{1/F}$, which is typical in regions of open-ocean convection—convective mixing yields local thermal anomalies and flow fields that are strongly confined within

the distance $O(L_R)$ to the vicinity of the location \mathbf{x}_i . Following the exchange of mass between the layers, the upper layer flow is cyclonic while the lower layer flow is anticyclonic. The effect of surface cooling over the basin is therefore well modeled by a superposition of heton structures in **10** with constant strengths, $\Delta q_i = \Delta Q$, independent of i , placed at random locations \mathbf{x}_i separated by L_R .

The heton strength, ΔQ , and the total amount of potential vorticity introduced into each layer of the fluid, $\Delta\Gamma$, are determined by the strength and duration of the surface cooling event, so that

$$\int q_1 = - \int q_2 = \Delta\Gamma. \tag{11}$$

Thus, $\Delta\Gamma$ depends on the total buoyancy lost over the cooling period. The statistical theory is based on these quantities, ΔQ , and $\Delta\Gamma$, together with the total energy, E , in the flow. We refer to ref. 3 for the detailed analytical formulas associated with the above heton model.

The link between the heton model and the equilibrium statistical theory is established by calculating the prior probability distributions for the potential vorticity in each layer, Π_{0j}^* , that are compatible with the heton forcing strength, ΔQ , and the total circulation, $\Delta\Gamma$, which is determined by a standard maximum entropy calculation (11). The result is the two probability densities for the microscale distribution of hetons,

$$\Pi_{0j}^*(\lambda) = \frac{e^{-\gamma_j \lambda} I_{Q_{j-}}^{Q_{j+}}(\lambda)}{\int e^{-\gamma_j \lambda} I_{Q_{j-}}^{Q_{j+}}(\lambda) d\lambda}, \quad j = 1, 2, \tag{12}$$

where $I_b^a(\lambda)$ represents a uniform distribution with unit area over the interval $[a, b]$, and Q_{j+} and Q_{j-} are the extrema for the potential vorticity in the j th layer induced by the heton forcing. In **12** the two constants, γ_j (with $\gamma_2 = -\gamma_1$), are determined uniquely by the conditions

$$\int \lambda \Pi_{0j}^*(\lambda) d\lambda = (-1)^{j+1} \Delta\Gamma, \quad j = 1, 2. \tag{13}$$

The probability measures, $\Pi_{0j}^*(\lambda)$, therefore encode the least-biased information given both the amplitude, ΔQ , and the total circulation strength, $\Delta\Gamma$, of the hetons.

We can interpret the prior probability measures in the following manner: pick the locations, \mathbf{x}_i , at random in the basin and pick the heton strengths, Δq_i at random from the probability distributions, $\Pi_{0j}^*(\lambda)$, and then the law of large numbers (12) guarantees that the probability measures, $\Pi_{01}^*(\lambda)$ and $\Pi_{02}^*(\lambda)$, given uniformly over the basin are well approximated by superpositions of random heton structures,

$$\begin{aligned} q_1 &= \frac{1}{N} \sum_{i=1}^N \Delta q_i \delta_{\mathbf{x}_i} \\ q_2 &= \frac{1}{N} \sum_{i=1}^N (-\Delta q_i) \delta_{\mathbf{x}_i}, \end{aligned} \tag{14}$$

for large enough values of N .

A schematic of the initial random heton ensemble is shown in Fig. 1. A measure of the statistical spreading of hetons is given by

$$\frac{\Delta\Gamma}{\Delta Q} = L_T^2, \tag{15}$$

which roughly quantifies the percentage area of the basin domain covered by hetons, so that $0 < L_T < 1$ (see, for example, Fig. 1).

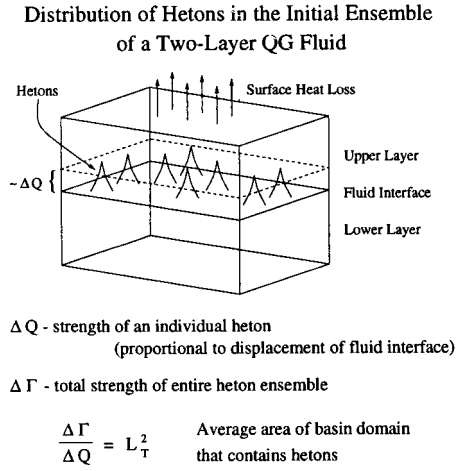


FIG. 1. A schematic showing the distribution of hetons in the initial ensemble. The heton strength parameter, ΔQ , is proportional to the displacement of the interface in a two-layer quasigeostrophic model. The length parameter, $L_T^2 = \Delta \Gamma / \Delta Q$, measures the average area of the unit basin that is initially seeded with hetons.

The Langevin Equilibrium Statistical Theory

Equilibrium statistical theories predict the long-term structures that arise at statistical equilibrium based on the conserved quantities contained in the initial flow. The key observation underlying the Langevin statistical theory is that physically useful results may be derived without accounting for all the vorticity invariants listed in 5. Recent numerical and theoretical considerations for damped and driven flows give strong support for utilizing only a few robust constraints such as the vortex extrema in each layer (8, 9), which for the heton ensemble described above are

$$\begin{array}{ll} \text{upper layer extrema} & 0, \quad \Delta Q \\ \text{lower layer extrema} & -\Delta Q, \quad 0. \end{array} \quad [16]$$

Here, we develop a statistical theory based on only a few constraints, i.e., from the energy, E , in 3, the circulations, $\Delta \Gamma$, in 4, and the extrema of the potential vorticities, in 16 (6, 7).

We achieve this through a coarse-graining procedure that replaces the fine-scale structure of the potential vorticity fields with statistical descriptions in terms of one-point probability distributions, $\rho_1(\mathbf{x}, \lambda)$ and $\rho_2(\mathbf{x}, \lambda)$, one for each layer, where the parameter λ varies over the range of potential vorticities. For any point \mathbf{x} in the basin domain and any two numbers, α_j and β_j , $\rho_j(\mathbf{x}, \lambda)$ describes the probability distributions of potential vorticity in each layer, i.e.,

$$\text{Prob}\{\alpha_j q_j(\mathbf{x}) \beta_j\} = \int_{\alpha_j}^{\beta_j} \rho_j(\mathbf{x}, \lambda) d\lambda, \quad j=1, 2. \quad [17]$$

As the fluid evolves into ever finer scales, which is typical of two-dimensional fluids, dominant mean-field potential vorticities, \bar{q}_1 and \bar{q}_2 , emerge on the largest scale, which are the solutions observed at long times. The one-point distributions and the most probable mean-field quantities are related by the *Mean-Field Equations*,

$$\bar{q}_j = \int \lambda \rho_j(\mathbf{x}, \lambda) d\lambda, \quad [18]$$

which together with the vorticity-stream function relations, 1, and the boundary conditions of no normal flow gives a coupled, nonlinear elliptic equation for the mean-field stream functions, $\bar{\psi}_1$ and $\bar{\psi}_2$.

To calculate the most probable state that emerges from a microscale distribution of hetons, we compute the one-point probability distributions, ρ_1 and ρ_2 , that maximizes the Shannon entropy, S , subject to the prior distributions in each layer, $\Pi_{01}^*(\lambda)$ and $\Pi_{02}^*(\lambda)$ (11),

$$\begin{aligned} S(\rho_1, \rho_2, \Pi_{01}^*, \Pi_{02}^*) \\ \equiv - \sum_{j=1}^2 \int \int \rho_j(\mathbf{x}, \lambda) \ln \frac{\rho_j(\mathbf{x}, \lambda)}{\Pi_{0j}^*(\lambda)} d\lambda dA. \end{aligned} \quad [19]$$

The distributions ρ_1 and ρ_2 are constrained by the energy, in 3, and probability measure definition, in 17.

The maximization of 19 subject to the constraints of energy and probability measure is solved by the method of Lagrange multipliers in the calculus of variations. We introduce the multiplier θ associated with the energy constraint. A standard calculation yields that for the most probable state, the probability densities in each layer take the form,

$$\rho_j(\mathbf{x}, \lambda) = \frac{e^{\theta \bar{\psi}_j \lambda} \Pi_{0j}^*(\lambda)}{\int e^{\theta \bar{\psi}_j \lambda} \Pi_{0j}^*(\lambda) d\lambda}, \quad j=1, 2. \quad [20]$$

The most probable coarse-grained state is found by substituting the probability distribution in 20 into the mean-field potential vorticities in 18. Upon substitution of the prior distributions shown in 12, the mean-field equations for a random heton ensemble in initially quiescent flow take the following form in the Langevin statistical theory,

$$\begin{aligned} \bar{q}_1 &= \frac{\Delta Q}{2} \left(1 + \mathcal{L} \left[\frac{\Delta Q}{2} (\theta \bar{\psi}_1 - \gamma_1) \right] \right) \\ &= \Delta \bar{\psi}_1 - F(\bar{\psi}_1 - \bar{\psi}_2) \\ \bar{q}_2 &= -\frac{\Delta Q}{2} \left(1 - \mathcal{L} \left[\frac{\Delta Q}{2} (\theta \bar{\psi}_2 - \gamma_2) \right] \right) \\ &= \Delta \bar{\psi}_2 + F(\bar{\psi}_1 - \bar{\psi}_2), \end{aligned} \quad [21]$$

which, along with the boundary conditions of no normal flow are a pair of coupled, nonlinear elliptic equations for the mean-field stream functions, $\bar{\psi}_j$. Here, we have $\mathcal{L}[x] \equiv \coth[x] - 1/x$, which is known as the Langevin function. Below we calculate the most probable states for the Langevin statistical theory by a maximum-entropy numerical procedure due to ref. 13.

Most Probable States for the Pure Heton Case

In this section we present the predictions of the equilibrium statistical theory for the spreading phase of a statistical ensemble of hetons distributed uniformly throughout a quiescent basin. Although the hetons are purely baroclinic and their placement is homogeneous, the maximum-entropy solution is typically a central monopole asymmetrically distributed between the two layers with roughly 90% of the energy budget being barotropic. The temperature anomaly, which is defined in 7, forms a relatively cool core that lies within the barotropic vortex, showing that hetons tend to cluster in the basin center, "governed" by the barotropic flow.

The scale of the vortices, both barotropic and baroclinic, are determined by two nondimensional length scales: $L_R = \sqrt{1/F}$, the Rossby deformation radius, and $L_T \equiv \sqrt{\Delta \Gamma / \Delta Q}$, which measures the density of hetons in the initial ensemble. For small values of the Rossby deformation radius, $L_R \ll 1$, which is typical for the sites of open-ocean convection (1), the statistical equilibrium flows establish a barotropic governor,

which is a barotropic rim current that confines the temperature anomaly and suppresses baroclinic instability. For increasing L_T the barotropic governor remains in place and provable nonlinear stability is established for a large range of L_T . For all solutions provided in this paper the heton strength is $\Delta Q = 2.0$, and the Rossby deformation radius is $L_R = 0.05$.

For small deformation radius, low heton density, $L_T = 0.19$, and moderate energies, $E \leq 0.00017$, the most probable states, which are calculated by solving the coupled mean-field equations in 21 for the upper- and lower-layer stream functions, are asymmetric monopoles. Thus, a random bombardment of baroclinically symmetric hetons in a uniform basin cooling event yields, at statistical equilibrium, an asymmetric arrangement of potential vorticity between the two layers. The potential vorticity accumulates in the center of the domain, with a broader cyclonic vortex in one layer and a more concentrated cyclonic vortex in the other, with nearly 90% of the energy budget being barotropic.

An example for $E = 0.000056$ is shown in Fig. 2. A more concentrated vortex appears in the upper layer and a broader vortex in the lower layer. The barotropic and baroclinic portions of the stream function show that the asymmetric monopole establishes, in the absence of any preexisting barotropic flow, its own barotropic governor. The extent of the barotropic stream function is broader than the baroclinic stream function, an effect that is illustrated by the relative widths of the stream function surfaces. Since the temperature anomaly is proportional to the baroclinic stream field by 7, this shows that the heat in the statistical equilibrium solution accumulates in a compact region in the center of the basin.

Effect of Heton Density on Most Probable States

For increasing L_T —i.e., raising the heton density in the original ensemble—both the barotropic and baroclinic portions of the equilibrium solutions spread. As the flow extends to the basin scale, the portion of the energy that is barotropic

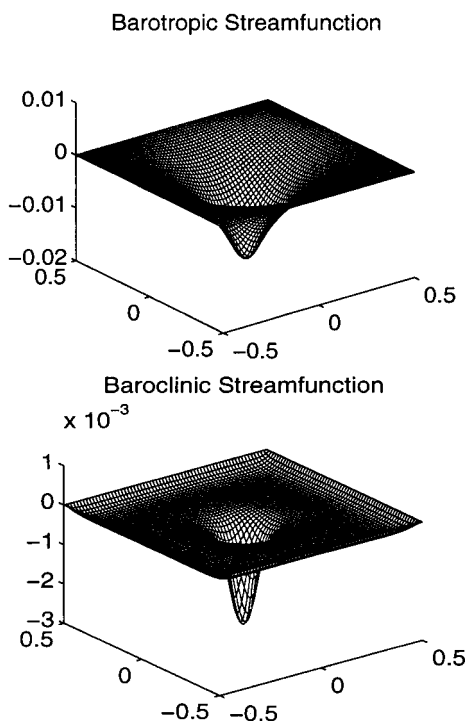


FIG. 2. Barotropic and baroclinic stream functions for the maximum-entropy asymmetric monopole for $L_R = 0.05$, $L_T = 0.19$, and $E = 0.000056$.

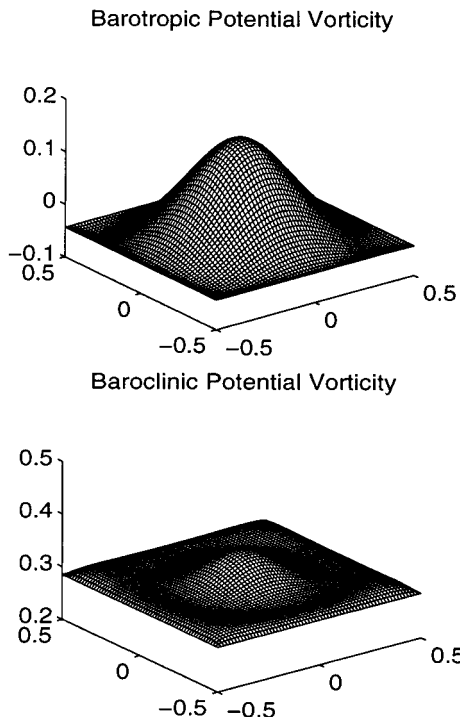


FIG. 3. Barotropic and baroclinic potential vorticity surfaces for $L_R = 0.05$, $E = 0.000156$, and $L_T = 0.39$. This example is nonlinearly stable.

decreases slightly, and provable nonlinear stability may be established for large enough L_T (14).

The most probable barotropic and baroclinic potential vorticity fields for deformation radius, $L_R = 0.05$, and energy, $E = 0.000156$, are shown in Fig. 3 for $L_T = 0.39$. In contrast to the example shown in Fig. 2, in which the potential vorticity fields are concentrated in the center of the basin, here the barotropic and baroclinic components of the potential vorticity extend to the basin scale. However, even as the equilibrium solutions spread with increasing L_T , the barotropic portions of the flow circumscribe the baroclinic fields and thus establish barotropic governors. For the example provided in Fig. 3, the length scale L_T is sufficiently large to ensure provable nonlinear stability.

Temperature anomalies for the same deformation radius and energy are shown in Fig. 4 A–C for $L_T = 0.19$, 0.27, and 0.39. An additional example is shown in Fig. 4D for a higher value of $L_T = 0.5$, and energy, $E = 0.0011$, which is provably nonlinearly stable. At small L_T , the hetons cluster into a sharply localized peak in the center of the basin. The fluid that surrounds the cold core is relatively flat, with an even distribution of heat. As the density of hetons in the initial ensemble increases, the magnitude of the anomaly decreases, the width of the core spreads, and the heat content in the surrounding flow increases, but remains uniformly distributed. The example shown in Fig. 4D demonstrates that a flow with significant cool thermal anomalies in the basin center can be nonlinearly stable (14).

Summary and Concluding Discussion

A “most probable state” equilibrium statistical theory for the spreading phase of open-ocean convection has been introduced and developed within the context of heton models for two-layer quasigeostrophic flow. The “most probable” equilibrium statistical states at large times are predicted through a maximum-entropy principle involving only a few judiciously chosen conserved quantities for the inviscid dynamics: energy, circulation, and extrema for potential vorticity in each layer.

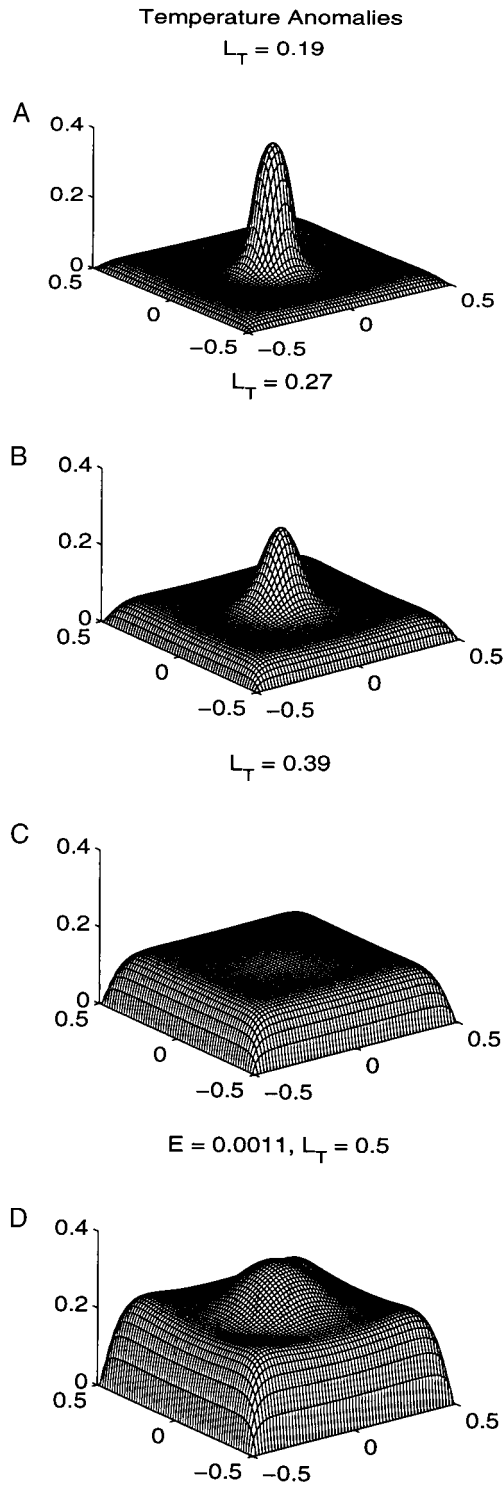


FIG. 4. Temperature anomalies for the asymmetric monopoles with $L_R = 0.05$, $E = 0.000156$, and $L_T = 0.19$ (A), 0.27 (B), and 0.39 (C). The final example in D has $E = 0.0011$ and $L_T = 0.5$. The two examples in the bottom row are both nonlinearly stable.

The statistical theory predicts the coarse-grained mean-field response to a random cooling event over the entire basin as represented by a random heton distribution with a prescribed maximum amplitude, ΔQ , and circulation anomaly, $\Delta \Gamma$.

For the situation with a small Rossby deformation radius compared to the basin scale, $L_R = 0.05$, the typical probable states are asymmetric monopoles with the overwhelming energy contribution being barotropic (85–90% of the energy budget) and the temperature anomaly confined within the region of strong barotropic flow. Thus, the statistical theory automatically predicts a confined temperature anomaly with a sheared rim current in qualitative agreement with numerical integration of heton models (3, 4). Also, the nonlinear stability of this predicted structure for fixed energy depends crucially on the size of the nondimensional parameter L_T , introduced in 15 with larger values yielding stability.

An important situation for further study involves the addition of a statistical ensemble of hetons, mimicking a cooling event, to a preexisting barotropic flow. Basin topography plays a significant role in the preconditioning for open-ocean convection (15, 16). An important future research direction is the influence of topography on the predictions of the equilibrium statistical theory as well as more general preexisting basin-scale flows. Another important research direction within the context of the two-layer models presented here involves the realizability and metastability of these equilibrium statistical steady states with damping and forcing representing wind stress. Such studies have already been developed elsewhere in simplified contexts (8, 9).

We thank John Marshall for his encouragement and helpful comments provided through the course of this work. M.T.D. is supported as a postdoctoral fellow at the Courant Institute by Grants NSF DMS-9625795 and ONR N00014-96-0043. The research of A.J.M. is partially supported by Grants ONR N00014-96-0043, NSF DMS-9625795, and ARO DAAG55-98-1-0129.

1. Marshall, J. & Schott, F. (1998) *Open-Ocean Convection: Observations, Theory and Models* (MIT Center for Global Change Science), Vol. 52, 1–146.
2. Hogg, N. G. & Stommel, H. M. (1985) *J. Atmos. Sci.* **42**, 1465–1476.
3. Legg, S. & Marshall, J. (1993) *J. Phys. Oceanogr.* **23**, 1040–1056.
4. Legg, S., Jones, H. & Visbeck, M. (1996) *J. Phys. Oceanogr.* **26**, 2251–2266.
5. Legg, S. & Marshall, J. (1998) *J. Mar. Res.* **56**, 107–139.
6. DiBattista, M. T., Majda, A. J. & Turkington, B. (1998) *Geophys. Astrophys. Fluid Dyn.* **89**, 235–283.
7. Turkington, B. (1999) *Comm. Pure Appl. Math.*, in press.
8. Majda, A. J. & Holen, M. (1997) *Comm. Pure Appl. Math.* **50**, 1183–1234.
9. Grote, M. J. & Majda, A. J. (1997) *Phys. Fluids* **9**, 3431–3442.
10. Pedlosky, J. (1979) *Geophysical Fluid Dynamics* (Springer, New York).
11. Jaynes, E. T. (1957) *Phys. Rev.* **106**, 620–630.
12. Lamperti, J. (1966) *Probability Theory* (Benjamin, New York).
13. Turkington, B. & Whitaker, N. (1996) *SIAM J. Sci. Comput.* **17**, 1414–1433.
14. Mu Mu, Zeng, Q., Shepherd, T. G. & Yongming, L. (1994) *J. Fluid Mech.* **264**, 165–184.
15. Hogg, N. G. (1973) *Deep-Sea Res.* **20**, 449–459.
16. Alverson, K. & Owens, W. (1996) *J. Phys. Oceanogr.* **26**, 2196–2213.